ISSN 0869-5911, Petrology, 2022, Vol. 30, Suppl. 1, pp. S53–S71. © Pleiades Publishing, Ltd., 2022.
Russian Text © The Author(s), 2023, published in Petrologiya, 2023, Vol. 31, No. 1, pp. 29–48.

Staurolite in Metabasites: *P–T–X* Parameters and the Ratios of Major Components as Criteria of Staurolite Stability

E. B. Borisova[a, b], *, **Sh. K. Baltybaev**[a, b], **, **and J. A. D. Connolly**[c]

[a] *Institute of Precambrian Geology and Geochronology, Russian Academy of Sciences, St. Petersburg, 190034 Russia*
[b] *St. Petersburg State University, St. Petersburg, 190034 Russia*
[c] *Earth Sciences Department, ETH, Zurich, Switzerland*
**e-mail: jenyaborisova98@gmail.com*
***e-mail: shauket@mail.ru*

Received March 18, 2022; revised May 12, 2022; accepted May 18, 2022

Abstract—Fe–Mg staurolite is a typical and widespread mineral of medium-temperature high-alumina metapelites, whereas magnesian staurolite is only relatively rarely found in metamorphosed mafic rocks (metabasites). The most significant factors controlling staurolite stability in metabasites were identified by thermodynamic modeling and analysis of the common features of the mineral-forming processes. In contrast to staurolite in low- and medium-pressure metapelites, staurolite in metabasites is stable at medium- and high-pressure metamorphism. An increase in the proportion of carbon dioxide in the water–carbon dioxide fluid shifts the staurolite-forming mineral reactions to lower temperatures and higher pressures. Al, Fe, Mg, and Ca are the major components of rocks that are critically important for the formation of magnesian staurolite in these rocks, and the contents and ratios of these components are of crucial importance for the stability of staurolite in metabasites. To understand the processes forming the mineral in metabasites, it is instrumental to subdivide metabasites into subgroups of predominantly magnesian, ferruginous–magnesian, and ferruginous protoliths. With regard to this subdivision, three petrochemical modules are proposed in the form of ratios of major components: MgO/CaO, CaO/FM, and Al_2O_3/FM, based on which it is possible to predict the stability of staurolite in mafic rocks at appropriate *P–T* parameters of metamorphism.

Keywords: staurolite, petrochemical module, metamorphism, mineral assemblages, thermodynamic modeling, fluid, metabasite

DOI: 10.1134/S0869591123010034

INTRODUCTION

The application of the petrochemical moduli Al_2O_3/SiO_2, CaO/FM[1], K_2O/FM, and Na_2O/FM makes it possible to predict the stability Fe–Mg staurolite in metapelites within given temperature and pressure ranges (Borisova and Baltybaev, 2021).

Ferro-magnesian staurolite is a widespread and typical mineral of medium-temperature aluminous metapelites, and magnesian staurolite is occasionally found in metamorphosed mafic rocks (metabasites) (Ríos et al., 2014 and references therein). Amphibolite-facies metabasites consist mostly of hornblende, plagioclase, and ±quartz and sometimes also contain chlorite, garnet, and epidote-group minerals, which are found more often than staurolite. Iron-rich amphibolites are commonly dominated by mineral assemblages of staurolite with garnet, whereas their more magnesian analogues contain chlorite and cordierite. Staurolite is sometimes found as an accessory mineral, together with kyanite, in corundum amphibolites.

Inasmuch as petrochemical moduli have been proved to be a promising and efficient tool in predicting staurolite mineral assemblages in metapelites of certain temperature and pressure ranges, it was natural to try to apply such moduli for predicting the stability of staurolite in mafic rocks. Below we use thermodynamic simulations to analyze the possibility of the stable crystallization of staurolite in metabasites at variations in the composition of the metamorphic fluid and concentrations of major components in the protoliths. Analysis of the *P–T–X* (pressure–temperature–composition) parameters of staurolite-forming processes led us to identify ratios of major oxides (petrochemical moduli) necessary for the stability of dominantly magnesian staurolite in metabasites.

Analysis of literature data allowed us to distinguish some factors necessary for stable staurolite crystallization in metabasites.

---

[1] FM = FeO_t + MgO.

Staurolite can be formed as a primary mineral in aluminous metabasites of the amphibolite metamorphic facies. It is believed that staurolite and kyanite (or sillimanite) can be formed in equilibrium with hornblende only at a certain bulk-rock composition (Spear, 1982; Purtscheller and Mogessie, 1984; Selverstone et al., 1984; Ward, 1984; Grew and Standiford, 1985) or at certain *P–T* parameters (Selverstone et al., 1984; Helms et al., 1987). Staurolite can be formed as a secondary mineral in high-pressure mineral assemblages of metabasites and replace chloritoid, corundum, and/or the garnet–kyanite assemblage. The mineral is also found as small inclusions in garnet (e.g., Enami and Zang, 1988).

Staurolite-bearing amphibolites can be formed via metasomatic exchange at contacts between pelite and calc-silicate rocks (Thompson, 1975; López and Soto, 1991; Ríos et al., 2008; Ríos and Castellanos, 2014). Staurolite metabasites can also be genetically related to aluminous and silicic rocks, as follows from the occurrence of mineral assemblages with kyanite, staurolite, and hornblende with identifiable clay or Ca-rich metamorphosed sediments (Spear, 1982; Selverstone et al., 1984; Ward, 1984; Humphreys, 1993; Kuhns et al., 1994).

Bearing in mind that the stable crystallization of staurolite may be controlled by numerous factors, we aimed at (i) identifying the most important major components of rocks that can control the stability of magnesian staurolite and (ii) at the more accurate evaluating of the *P–T–X* crystallization parameters of the mineral in mafic metamorphic rocks. We have conducted thermodynamic simulations and derived petrochemical moduli required for the stability of staurolite, using samples of naturally occurring rocks that are comprehensively described in the literature.

FACTUAL MATERIALS AND METHODS

The main method we applied to analyze the mineral assemblages of staurolite was numerical simulations of the mineral-forming processes by means of minimizing the Gibbs free energy with the PERPLEX v. 6.91 software (Connolly, 1990, with updates at 2021, www.perplex.ethz.ch). The simulations were carried out using the hp62ver.dat (Holland and Powell, 2011) thermodynamic database for minerals and solid solutions, which includes actual thermodynamic parameters for plagioclase, amphiboles, biotite, garnet, spinel, olivine, orthopyroxene, omphacite, talc, chlorites, white micas, chloritoid, staurolite, cordierite, and ilmenite in the system MnNCKFMASH ($MnO–Na_2O–CaO–K_2O–FeO–MgO–Al_2O_3–SiO_2–H_2O–CO_2$).

To constrain the ranges of metabasite compositions potentially suitable for staurolite stability in them, we used amphibolites (six samples) in which staurolite has been unambiguously identified (Purttscheller and Mogessie, 1984; Enami and Zang, 1988; Gil Ibarguchi et al., 1991; Tsujimori and Liou, 2004; Faryad and Hoinkes, 2006) and approximately 150 additional analyses to expand the ranges of the real amphibolite compositions (Fig. 1). These additional compositions allowed us to more accurately determine the threshold values of concentrations of various major components that are critical for staurolite stability in the tested rocks. The applicability and validity of this approach has been tested in (Borisova and Baltybaev, 2021).

Although staurolite in metabasites was documented in numerous publications, we have constrained our choice of rocks to correspond as closely as possible to the term *metabasite* as a rock with SiO_2 < 52 wt % and CaO > 5 wt %. These compositions are referred to as *basic* below.

To identify the compositions of the protoliths of the metabasites in which staurolite can be formed, the chosen basic compositions were modified by sequentially increasing or decreasing their major oxide by as much as 20 wt % from the original (unmodified) compositions of these rocks. For all basic and modified rock compositions, pseudosections were computed at $T = 500–800°C$ and $P = 1–38$ kbar. Thermodynamic simulations of mineral-forming processes with the use of a broad spectrum of sample compositions allowed us to constrain the threshold concentrations of major oxides that control the stability of staurolite-bearing and staurolite-free mineral assemblages in the specified *P–T* field.

In simulating equilibria between mineral phases with the PERPLEX software (Connolly, 1990), the input data were chemical analyses of metabasites (Table 1). When solving the direct modeling problem to reproduce naturally occurring mineral assemblages based on a specified composition of a rock and *P–T* parameters, we assumed that the system contains either pure H_2O or $H_2O–CO_2$ fluid. For the latter, we recalculated the phase diagrams by stepwise adding (with increments of 0.2) CO_2 to the fluid to a maximum CO_2 mole fraction of 0.8, a value above which ($X_{CO_2} > 0.8$) staurolite ceases to remain stable in any rocks in the whole spectrum of the studied compositions.

Rocks

This section summarizes the characteristics of the rocks that were identified as having basic composition. Note that we have compiled literature data on the compositions of amphibolites in which staurolite was found and identified and for which staurolite stability was proved by thermodynamic simulations. The diversity of tectonic settings in which staurolite-bearing amphibolites were found predetermines the broad ranges of *P–T* parameters in which these rocks can be formed.

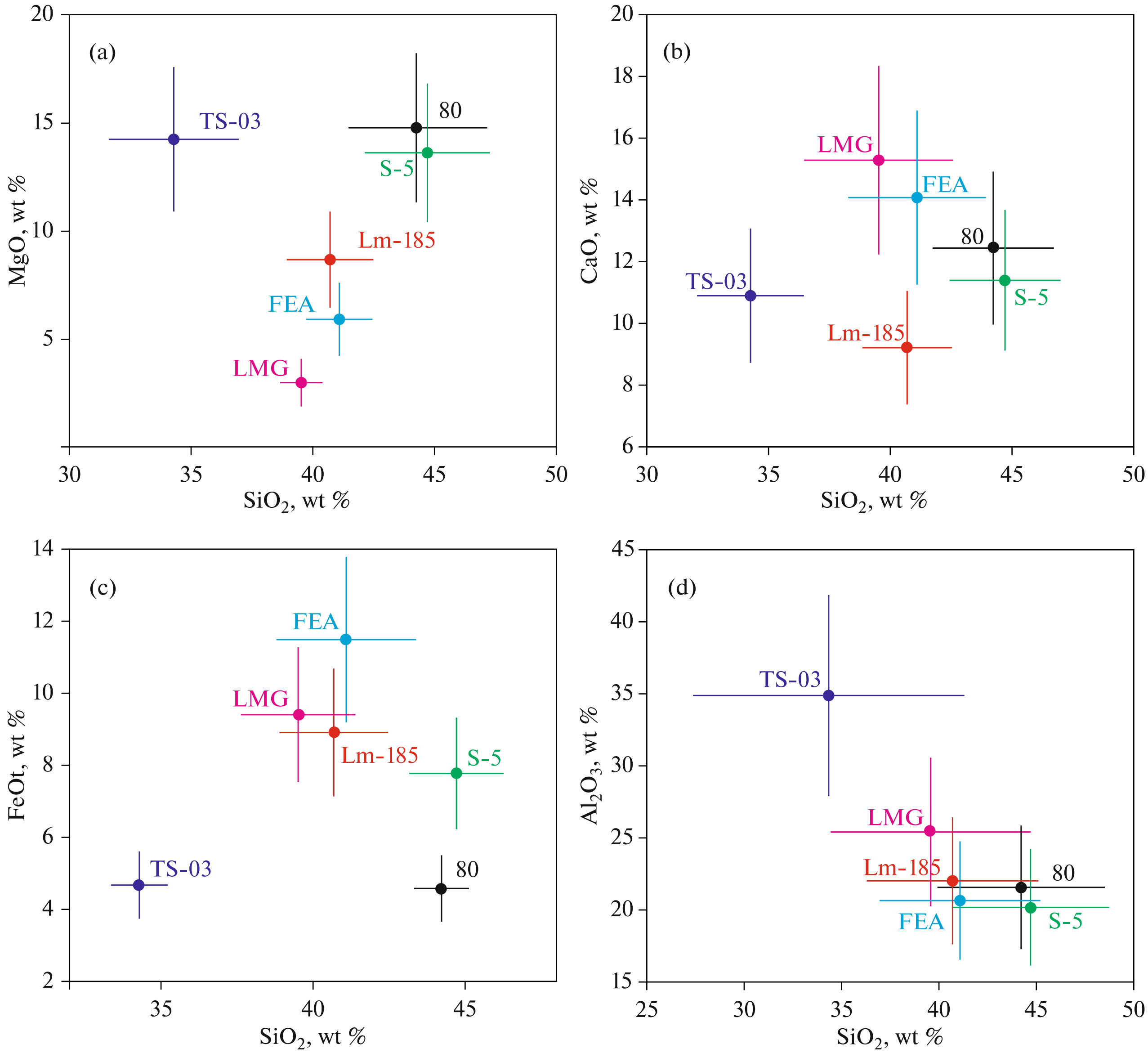

Fig. 1. (a) $MgO–SiO_2$, (b) $CaO–SiO_2$, (c) $FeO_t–SiO_2$, (d) $Al_2O_3–SiO_2$ diagrams for staurolite-bearing metabasites. Data points correspond to the composition of natural rocks from which the theoretical compositions were calculated, and the ranges are shown with horizontal and vertical bars.

Sample Lm-185 (Faryad and Hoinkes, 2006) is an aluminous amphibolite from the Speik complex in the Eastern Alps, which contains coexisting kyanite, staurolite, garnet, and calcic amphibole. Textural features of the minerals, mineral thermobarometry, and thermodynamic simulations suggest that the rock was affected by prograde metamorphism to the high-pressure amphibolite facies ($P = 11–12$ kbar, $T = 580°C$) and was affected by subsequent decompression to 5 kbar. The sample was taken from the central part of the metabasite belt of the Speik complex, but it is uncertain whether its high alumina concentration is primary or resulted from overprinted hydrothermal alterations before the amphibolite-facies metamorphic event. If the protolith of the rock was of magmatic nature, it corresponded to gabbro. The rock is coarse-grained, with large garnet porphyroblasts, but without garnet where the rock is sheared. The rock consists of amphibole (close to 58 vol %), garnet (14 vol %), clinozoisite (6 vol %), plagioclase (5 vol %), margarite + muscovite (8 vol %), chlorite (5 vol %), kyanite (4 vol %) and accessory staurolite, with some other minerals found as inclusions in garnet. Textural relationships seen in this rock indicate that it has been formed by four pulses of mineral-forming processes: prograde metamorphism (*Grt*[2] + *Ky* + *St* + *Kfs*? + *Rt* + *Tur* +

---

[2] Mineral symbols are according to (Whitney and Evans, 2010).

Table 1. Concentration of major components (wt %) in the rocks of the metabasite group

Oxide	Composition of natural staurolite-bearing metabasites			Theoretical compositions			
	group 1 (Fe/Mg ≪ 1)	group 2 (Fe/Mg ~ 1)	group 3 (Fe/Mg ≫ 1)	All	Max/Min	Only *St*-bearing	Max/Min
SiO_2	42.55	40.88	43.80	40.73	*48.73*	40.88	*48.73*
	4.13	0.20	4.29	3.09	*27.31*	3.06	*30.79*
Al_2O_3	22.67	21.31	23.84	24.11	*41.84*	24.20	*38.36*
	6.10	0.68	1.63	4.17	*16.14*	4.11	*16.14*
FeOt	6.19	10.21	10.19	7.80	*13.80*	7.60	*11.50*
	1.57	1.29	0.79	2.18	*3.66*	2.16	*3.66*
MnO	0.15	0.21	0.18	0.16	*0.25*	0.16	*0.25*
	0.05	0.05	0.07	0.05	*0.07*	0.05	*0.07*
MgO	13.61	7.84	3.49	9.95	*16.60*	10.05	*15.21*
	0.46	1.10	0.89	3.33	*3.50*	3.29	*3.50*
CaO	12.06	11.64	9.91	12.22	*18.35*	12.14	*18.35*
	0.91	2.44	5.38	1.81	*7.36*	1.83	*7.36*
Na_2O	0.90	1.52	0.83	1.12	*2.21*	1.08	*2.21*
	0.42	0.32	0.08	0.45	*0.12*	0.43	*0.12*
K_2O	0.19	0.68	0.61	0.46	*1.89*	0.47	*1.89*
	0.15	0.32	0.03	0.24	*0.00*	0.26	*0.00*
P_2O_5	0.11	0.08	0.04	0.10	*0.33*	0.11	*0.33*
	0.11	0.03	0.03	0.08	*0.00*	0.08	*0.00*
TiO_2	0.32	0.77	0.76	0.45	*0.78*	0.44	*0.78*
	0.27	0.01	0.26	0.27	*0.02*	0.28	*0.02*
Number of samples	4	2	2	144		90	

For natural samples, numerators list the arithmetic mean values, and denominators are the mean square deviation values. For theoretical ("expanded") compositions, numerals in italics in numerates are the maximum concentrations of the components, and numerals in denominators are the minimum values.

Ap + *Amp* + *Ep* + *Ms*?) and three episodes of retrogression. The absence of cordierite from this rock indicates that the maximum temperature at decompression to 6.5 kbar was lower than 590°C (Faryad and Hoinkes, 2006).

The staurolite of this rock is Fe-rich: $X_{Mg} = 0.21$–24. The ZnO concentration of this mineral is very low, 0.13 to 0.47 wt %, which corresponds to 0.013–0.046 Zn p.f.u.[3] The mineral always contains minor concentrations of Mn and Ti (no more than 0.4 wt %).

Sample S-5 (Purttscheller and Mogessie, 1984) is staurolite-bearing garnet amphibolite (*St* + *Hbl* + *Grt* + *Ky*) from the Ötztal Alps. The rock was affected by Hercynian metamorphism to P = 3–4 kbar, T = 670°C. The protolith of the rock is of reportedly undoubted magmatic nature. The rock contains staurolite as small (2–10 nm) inclusions of acicular crystals in hornblende and garnet and, mostly, as such crystals at contacts of these minerals. The staurolite has $X_{Mg} = 100\ Mg/(Mg + Fe) = 0.32$, which is higher than that of this mineral in metapelites ($X_{Mg} = 0.21$). All other compositional characteristics of the staurolite are the same as those of this mineral in metapelites. We are in doubt as to whether these authors have accurately and realistically evaluated the metamorphic parameters of the rock, but nevertheless, we use the analysis of this sample to cover as much as possible the compositions of the protoliths whose metamorphism might have resulted in staurolite-bearing rocks.

Sample TS-03 (Enami and Zang, 1988) is a garnet–corundum rock that contains magnesian (X_{Mg} = 0.68–0.74) staurolite and was found as isolated blocks in an ultramafic complex emplaced into Precambrian pelitic gneisses in the Donghai district, Jiangsu province, east China. The rock is dominated by garnet and

---

[3] p.f.u. is the number of ions per formula unit.

corundum and contains some amounts of zoisite and sodic phlogopite, along with secondary magnesian staurolite, chlorite, aluminous pargasite, clinozoisite, and magnesian allanite. The corundum hosts fine-crystalline inclusions of aggregates of diaspore, margarite, dolomite, and calcite (<0.03 mm). The equilibrium crystallization conditions of the primary assemblage were evaluated at $T = 800$–850°C, $P = 11$–30 kbar. The Mg-staurolite occurs as acicular and/or prismatic crystals and pseudomorphs after garnet and corundum with chlorite, which were formed according to the reaction *Grt* + *Crd* + H_2O = Mg-*St* + *Chl*. The equilibrium crystallization pressure of the staurolite was evaluated at >11 kbar, whereas the equilibrium temperature was slightly lower than that of the primary assemblage.

The rock has a very high Al_2O_3/SiO_2 ratio and a low FeO_t (4.7 wt %), which makes this chemical composition close to that of diaspore bauxite. The rock is also relatively rich in MgO and CaO, whose concentrations are explained by the authors as related to dolomite and limestone in association with the bauxite. Similar to the composition of the previous sample, we used the composition of this one to as widely as possible cover of protolith compositions in which staurolite can be formed at metamorphism.

Sample LMG, FEA (Tsujimori and Liou, 2004) is kyanite–staurolite–epidote amphibolite from a metacumulus sequence of the Fuko Pass in the Oeyama belt, southwestern Japan. The rocks are leucocratic metagabbro that consists mostly of clinozoisite and kyanite with subordinate amounts of hornblende, margarite, paragonite, staurolite, rutile, chlorite, zoisite, and muscovite; the accessory minerals are ilmenite and apatite. Evidence of the following three metamorphic events was identified in the rocks: relics of granulite-facies metamorphism *Cpx* + *Pl* + *Spl* ± *Opx* (M1), of the high-pressure epidote-amphibolite facies *Hbl* + *Czo* + *Ky* + *St* + *Pg* + *Rt* ± *Ab* ± *Crn* (M2), and of retrogression when margarite, paragonite, muscovite, chlorite and sometimes plagioclase pseudomorphs were formed (M3). The metamorphic peak parameters were evaluated at $P = 11$–19 kbar, $T = 550$–800°C. The coarse-crystalline clinozoisite (up to 15 mm) hosts inclusions of all M2 minerals. The staurolite has $X_{\mathrm{Mg}} = 0.16$–0.29 and contains ZnO = 0.9–2.0 wt %. Sample FEA differs from LMG in that the former is more intensely sheared.

Sample 80 (Gil Ibarguchi et al., 1991) is a kyanite–staurolite ultramafic rock that was found as lenses (10 × 1 m) in eclogites (whose composition is close to N-MORB) in the Cabo Ortegal complex in northwestern Spain. The parameters of metamorphism to the eclogite facies were evaluated at $T =$ 800°C, $P > 17$ kbar. The kyanite–staurolite rock shows a mineral lineation accentuated by elongate amphibole, zoisite, and kyanite crystals, with this lineation coinciding with that in the eclogite (due to elongate omphacite crystals). The primary phases other than hornblende, zoisite, and kyanite are garnet, staurolite, and spinel. This rock is unusual in that its kyanite and staurolite are enriched in Cr to 4.35 wt % and 6.4 wt %, respectively. The staurolite has $X_{\mathrm{Mg}} = 0.58$–0.74.

SIMULATION OF THE MINERAL-FORMING PROCESSES: NATURAL AND THEORETICAL METABASITE COMPOSITIONS

Effect of the Protolith Composition

Our simulation results show that the mineralogical composition of the metabasites strongly depends on the chemical composition of their protoliths. Variations were identified both in the number of the modeled P–T fields of mineral assemblages with staurolite and in the configuration and size of these fields. To generalize the results and identify the leading trends in the mineral-forming processes, the compositions of the metabasites were classified according to their concentrations of major components able to affect staurolite stability. The most informative compositions were those of samples 80, LMG, and Lm-185, which notably differ from one another in the FeO_t/MgO and Al_2O_3/MgO ratios. Below we discuss mineral-forming processes in both the starting compositions of the rocks and in these compositions variably modified.

Sample 80. The following three fields of staurolite-bearing mineral assemblages were simulated for the original composition of sample 80 (Fig. 2, gray fields): (1) a higher pressure region, $P = 26$–29 kbar ($T =$ 630–690°C), in which such high-pressure minerals are present as omphacite and lawsonite, including accessory rutile: *St* + *Grt* + *Amp* + *Cpx* + *Bt* ± *Tlc* ± *Chl* ± *Ky* ± *Lws* ± *Zo* ± *Rt;* (2) a field significantly stretching along the pressure axis, $P = 11$–20 kbar ($T = 670$–700°C), which is characterized by the dominance of talc and the absence of high-pressure minerals but the presence of muscovite: *St* + *Grt* + *Amp* + *Zo* ± *Bt* ± *Tlc* ± *Chl* ± *Ms* ± *Ky;* and (3) the smallest field, $P = 8$–10 kbar ($T = 690$–730°C), in which plagioclase is stable: *St* + *Grt* + *Amp* + *Pl* ± *Chl* ± *Ms.*

Effect of the bulk-rock Al_2O_3 concentration on staurolite stability (Fig. 2a). At $P = 27$ kbar, $T = 660$°C, and the original (unmodified) rock composition, this rock is dominated by garnet and clinopyroxene and contains subordinate amounts of staurolite, kyanite, biotite, and zoisite (in vol %): *St* 4.92, *Grt* 53.79, *Cpx* 30.38, *Ky* 4.73, *Bt* 4.43, *Zo* 1.94. The staurolite is mostly magnesian ($X_{\mathrm{Mg}\text{-}St} = 0.89$), with $X_{\mathrm{Fe}\text{-}St} = 0.06$ and has a much lower Mn mole fraction of 0.001. The garnet is pyrope rich in the grossular component and contains relatively little almandine ($Prp_{0.55}Grs_{0.29}Alm_{0.15}Sps_{0.002}$). The clinopyroxene is dominated by diopside (Ca–Mg pyroxene), $X_{Di} = 0.71$, and contains less of the jadeite component (Na–Al pyroxene), $X_{Jd} = 0.21$, and much less hedenbergite (Ca–Fe *Cpx*), $X_{Hed} = 0.01$. The bio-

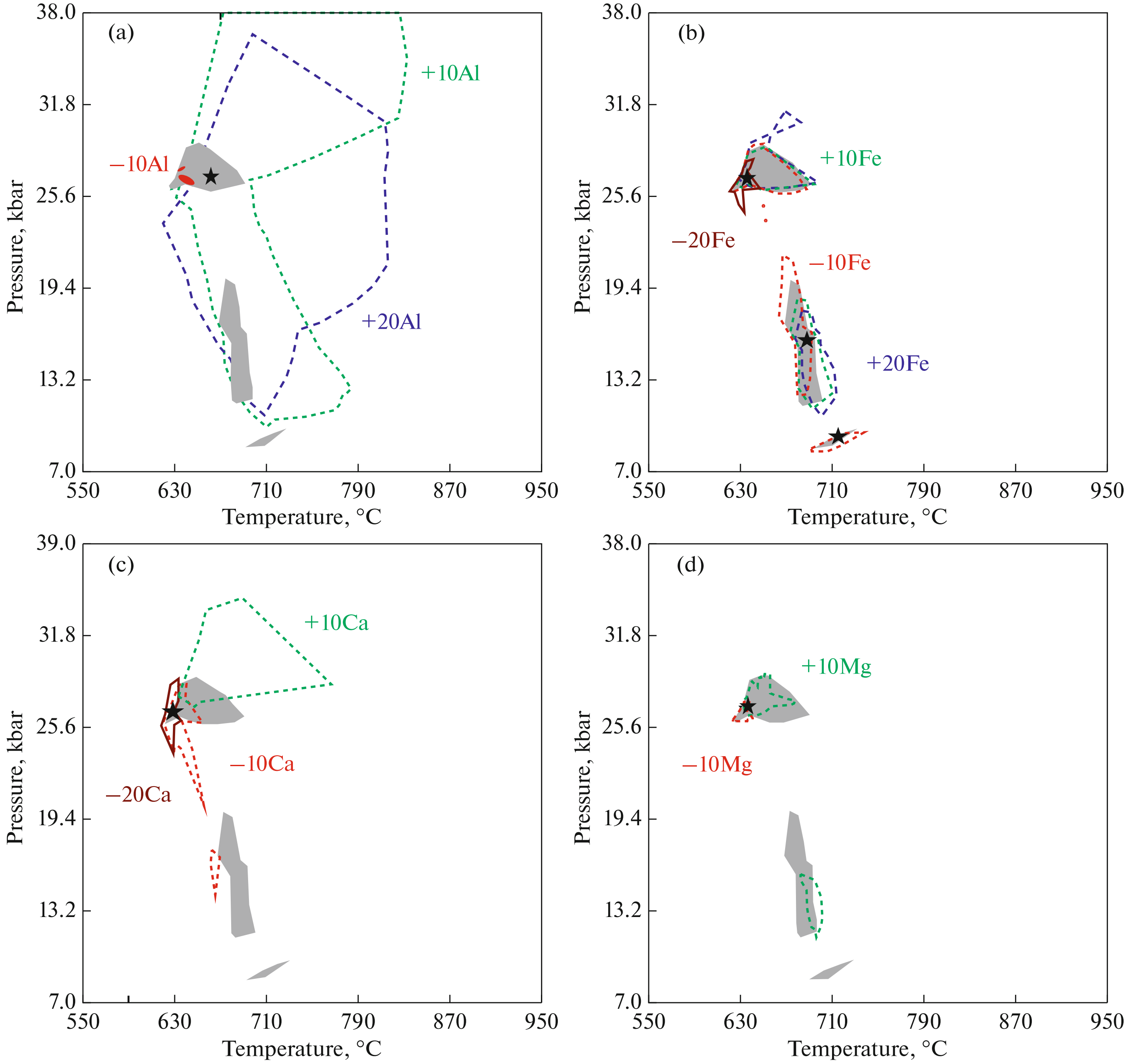

Fig. 2. Changes in the configurations of staurolite stability fields in *P–T* diagrams with variations in the concentrations of major components in the protolith. The basic composition of the metabasite was assumed to be that of sample 80. (a) Al_2O_3, (b) FeO_t, (c) CaO, (d) MgO, where «+10», «+20», «−10», and «−20» mean the increase or decrease in the content of the respective component by 10 or 20% relative to the original (unmodified) composition of the rock. Gray fields are the fields with staurolite at the unmodified composition of the rock, green lines contour fields at the addition of 10% of the components, blue lines correspond to the addition of 20%, and red and brown ones pertain to a decrease by 10 and 20%, respectively.

tite is phlogopite ($X_{Phl} = 0.77$) that is relatively poor in the eastonite end member ($X_{Eas} = 0.08$), even poorer in the Ti-biotite end member ($X_{\text{Ti-}Bt} = 0.07$), much poorer in the annite ($X_{Ann} = 0.02$), and Fe−Mg biotite ($X_{\text{Fe}^{2+}\text{-Mg}} = 0.04$) components.

An increase in the Al_2O_3 concentration (from −10Al to +20Al) leads to a significant expansion of the staurolite stability fields and their mergence into a single field. At constant *P–T* parameters ($P = 27$ kbar, $T = 660$°C), the rock enriches in garnet (from 49 to 57 vol %) and staurolite (up to 7.4 vol %) but reduces clinopyroxene abundance from 34 vol % to zero when amphibole is formed (up to 23 vol %). Therewith kyanite decomposes and zoisite and chlorite are formed. An increase in the X_{Mg} of the staurolite[4]

---

[4] The coupled variations in the X_{Mg} of the minerals are discussed in more detail below.

($X_{Mg\text{-}St}$ = 0.81–0.92) is associated with a decrease in that of the garnet (to $Prp_{0.45}$). A 10% decrease in the Al_2O_3 concentration from the original composition results in a significant shrinkage of the fields of the staurolite-bearing assemblages, and no staurolite is formed at all when the Al_2O_3 is further decreased.

Changes in the Al_2O_3 concentration thus strongly affect the configuration of the *P*–*T* region of staurolite stability in mafic rocks and is one of the most important parameters of staurolite stability.

Effect of the bulk-rock FeO_t concentration on staurolite stability (Fig. 2b). At *P* = 27.15 kbar, *T* = 635°C, and the unmodified composition of the rock, this rock is dominated by garnet and clinopyroxene and contains much biotite, talc, zoisite, and chlorite. The rock contains relatively much staurolite (in vol %): *St* 7.99, *Grt* 44.48, *Cpx* 25.61, *Bt* 4.32, *Tlc* 5.42, *Zo* 9.71, and *Chl* 2.48. The staurolite is magnesian: $X_{Mg\text{-}St}$ = 0.89, $X_{Fe\text{-}St}$ = 0.07. The garnet is pyrope that is rich in grossular and contains a little almandine: $Prp_{0.52}Grs_{0.30}Alm_{0.18}Sps_{0.003}$. The clinopyroxene has a dominantly Ca–Mg composition, X_{Di} = 0.61, X_{Jd} = 0.19, and X_{Hed} = 0.01. The biotite is phlogopite, X_{Phl} = 0.80, X_{Eas} = 0.06, X_{Ann} = 0.02.

An increase in the FeO_t content of the rock leads to a decrease in the amount of staurolite at high pressures (from 8 to 3 vol %) and a small decrease in its X_{Mg} from 0.89 to 0.85. At the same time, the content of garnet in the rock increases from 44 to 53 vol % without any significant changes in its composition. At +10Fe, chlorite is formed, and a further increase in the content of FeO_t leads to an increase in its content in the rock (to 7.8 vol %).

With decreasing FeO_t of the rock, the content of staurolite in the rock remains close to 8 vol %, whereas a decrease in FeO_t by 20% leads to a decrease in its content to 1.5 vol %, and the X_{Mg} of the staurolite simultaneously drops from 0.89 to 0.83. The same pertains to the clinopyroxene: its amount decreases from 26 to 15 vol %. The content of magnesian talc increases from 5 to 23 vol %, and the content of zoisite increases from 10 to 24 vol %. At –20Fe, kyanite is formed, seemingly because alumina is released.

A decrease in the FeO_t content of the rock results in a decrease in the staurolite content at *P* = 11–20 kbar (up to the complete absence of this mineral), the content of garnet simultaneously decreases from 17 to 7 vol %, the amphibole amount decreases from 57 to 44 vol %, and biotite disappears. Therewith the contents of talc and zoisite increase, and muscovite, kyanite, and quartz are formed. The garnet simultaneously depletes in the pyrope component.

The mineral assemblage at *P* = 8–10 kbar consists of amphibole and a dominant amount of plagioclase (anorthite), garnet, and staurolite. The staurolite is notably ferrous ($X_{Mg\text{-}St}$ = 0.76). A 10% decrease in the FeO_t content results in that muscovite is formed.

An increase in the FeO_t content (from −10Fe to +20Fe) and the transition from high to intermediate pressures result in that the staurolite field is slightly shifted, and at low pressures, staurolite disappears at +10Fe. Changes in the FeO_t content generally do not affect the location and size of the staurolite fields as significantly as Al_2O_3 concentrations do.

Effect of the bulk-rock CaO concentration on staurolite stability (Fig. 2c). At *P* = 28.5 kbar, *T* = 640°C, and the unmodified rock composition, the rock consists of the following mineral assemblage (in vol %): *St* 3.64, *Grt* 55.43, *Cpx* 24.00, *Lws* 12.07, *Bt* 4.32, *Tlc* 0.54.

An increase in the CaO content by 10% results in that talc and lawsonite disappear from the assemblage and instead chlorite and zoisite are formed. The staurolite content dramatically decreases from 3.4 to 0.4 vol %, and the mineral becomes less magnesian from 0.88 to 0.84. The amount of garnet increases, with simultaneous increase of the grossular component from 0.28 to 0.36. The clinopyroxene content decreases from 24 to 17 vol %, and it strongly depletes in the diopside component, from 0.57 to 0.29.

At decreasing CaO content by 10%, the amount of staurolite decreases from 3.6 to 1.1 vol %, which is accompanied by the decrease of its X_{Mg} from 0.88 to 0.82. The amount of garnet and omphacite also decreases, while that of lawsonite and talc, increases.

A change in the CaO content notably modifies the configurations of the fields of staurolite stability. At an insignificant increase in the CaO content, the field with staurolite expands at high pressures, but starting with a certain CaO concentration, no staurolite is formed in the rock any more. A decrease in the CaO concentration is less critical for a change in staurolite stability, although there seems to be a tendency toward staurolite disappearance from the low-pressure portion of the diagram.

Effect of the bulk-rock MgO concentration on staurolite stability (Fig. 2d). At *P* = 27.3 kbar, *T* = 635°C, and the unmodified composition of the rock, it is dominated by garnet and clinopyroxene and contains much biotite, talc, and zoisite. The rock contains relatively much staurolite (in vol %): *St* 11.11, *Grt* 45.50, *Cpx* 30.14, *Bt* 4.37, *Tlc* 3.68, and *Zo* 5.20. The staurolite is magnesian, $X_{Mg\text{-}St}$ = 0.90, $X_{Fe\text{-}St}$ = 0.06. The garnet is pyrope rich in grossular and poor in almandine: $Prp_{0.52}Grs_{0.30}Alm_{0.18}Sps_{0.003}$. The clinopyroxene is of Ca–Mg composition, X_{Di} = 0.70, X_{Jd} = 0.20, X_{Hed} = 0.01. The biotite is phlogopite, X_{Phl} = 0.80, X_{Eas} = 0.07, X_{Ann} = 0.02.

At an increase in the MgO content by 10%, the content of staurolite in the rock significantly decreases, from 11 to 3 vol %, and its X_{Mg} therewith decreases from 0.9 to 0.86. Simultaneously the content of clinopyroxene decreases, talc disappears, and chlorite is formed (up to 16 vol %) because of the increase in MgO content. A further increase in the MgO content is not associated with the crystallization of staurolite, the amount of garnet and omphacite thereby decrease, and that of chlorite strongly increases up to 32 vol %. Simultaneously, the X_{Mg} of garnet decreases, the *Prp* concentration decreases from 0.51 to 0.39, and the clinopyroxene therewith significantly depletes in the diopside component, from 0.50 to 0.24.

A decrease in the MgO content by 10% leads to a drastic decrease in the staurolite content from 11 to 0.6 vol %, and its X_{Mg} thereby significantly decreases to 0.81. The decrease in the clinopyroxene content is associated with that lawsonite is formed in the mineral assemblage. Neither the composition of the garnet nor its content are therewith changed any significantly. No staurolite is formed with a further decrease in MgO content in the rock, the content of garnet decreases from 42 to 32 vol %, the lawsonite content increases to 31 vol %, and muscovite is formed in the rock. The concentration of the pyrope component in the garnet decreases from 0.51 to 0.46.

In general, both an increase and a decrease in MgO content in the rock by 10% leads to a significant shrinkage of the stability fields of staurolite and its content in the rock. At −20Mg, +20Mg, no staurolite is formed at all.

Sample LMG. For the composition of amphibolite LMG (Tsujimori and Liou, 2004), staurolite-bearing mineral assemblages occur at high pressures (P = 25–37 kbar, T = 610–720°C) and are characterized by the presence of such high-pressure minerals as omphacite, lawsonite, and kyanite: *St* + *Grt* + *Cpx* + *Ms* + *Rt* ± *Bt* ± *Lws* ± *Amp* ± *Crn* ± *Zo* ± *Ky* (Figs. 3a–3d).

Effect of the bulk-rock Al_2O_3 concentration on staurolite stability (Fig. 3a). At P = 30 kbar, T = 670°C, and the unmodified composition of the rock, it is dominated by garnet and zoisite and contains smaller amounts of clinopyroxene, muscovite, and staurolite (in vol %): *St* 3.96, *Grt* 61.19, *Zo* 19.65, *Cpx* 8.00, *Ms* 6.78, *Rt* 0.42. The staurolite has $X_{\mathrm{Mg}\text{-}St}$ = 0.68, $X_{\mathrm{Fe}\text{-}St}$ = 0.23. The garnet is dominated by grossular and contains lower concentrations of almandine and pyrope and practically no spessartine ($Prp_{0.23}Grs_{0.46}Alm_{0.31}Sps_{0.003}$). The clinopyroxene is jadeite X_{Jd} = 0.80 and is poor in the diopside component X_{Di} = 0.11.

An increase in the Al_2O_3 content by 10% relative to the unmodified composition results in an increase in the staurolite content in the rock from 4 to 7 vol % and in the crystallization of corundum in this rock. The composition of minerals in the assemblages thereby does not change. No staurolite is formed in the rock at a further increase in the Al_2O_3 concentration, muscovite becomes unstable, and corundum and biotite are formed instead of it. A decrease in the Al_2O_3 content by 10% leads to the disappearance of staurolite and the appearance of lawsonite and coesite.

Effect of the bulk-rock FeO_t concentration on staurolite stability (Fig. 3b). At P = 29.5 kbar, T = 640°C, and the unmodified composition of the rock, it is dominated by garnet and zoisite and consists of the following assemblage (in vol %): *St* 4.06, *Grt* 61.16, *Zo* 19.60, *Cpx* 8.01, *Ms* 6.73, *Rt* 0.42, *Bt* 0.01. The garnet is mostly grossular with lower concentrations of almandine and pyrope. The staurolite is magnesian: $X_{\mathrm{Mg}\text{-}St}$ = 0.69. The clinopyroxene is jadeite.

An increase in the FeO_t content by 10% leads to an increase in the staurolite content from 4 to 6.5 vol % and a decrease in its X_{Mg} from 0.69 to 0.63. The content of biotite decreases up to its virtually complete disappearance, but corundum is therewith formed. The garnet becomes depleted in pyrope (from 0.23 to 0.18) and enriched in grossular (from 0.46 to 0.49) and almandine (from 0.31 to 0.33). The clinopyroxene becomes depleted in the diopside end member and enriched in the jadeite component. A further increase in the FeO_t content by 20% results in a significant decrease in the staurolite content to 0.12 vol % and an increase in the garnet content to 70 vol %. No other critical changes in this mineral assemblages were detected.

A decrease in the FeO_t content by 10% leads to a decrease in the staurolite content in the rock from 4 to 0.6 vol %, a decrease in the garnet amount, and the disappearance of biotite and appearance of lawsonite. The X_{Mg} of both the staurolite and the garnet slightly increases. A further decrease in the FeO_t content results in that no staurolite is formed in this rock.

Effect of the bulk-rock CaO concentration on staurolite stability (Fig. 3c). An increase in the CaO content by 10% (from 15.3 to 16.8 wt %) completely suppresses staurolite, and the following staurolite-free mineral assemblage is stable at P = 30.6 kbar, T = 650°C (in vol %): *Grt* (66.1) + *Cpx* (7.8) + *Bt* (6.7) + *Zo* (31.1) + *Rt* (0.4) + *Crn* (3.1). The content of zoisite increases, as also does Ca concentration in the garnet, and biotite is formed instead of muscovite.

A decrease in the CaO concentration by 10% (to 13.76 wt %) leads to the practically complete disappearance of staurolite from the rock, and the following mineral assemblage thus "remains" at P = 25.8 kbar, T = 610°C: *St* + *Grt* + *Cpx* + *Ms* + *Rt* ± *Bt* + *Lws* + *Zo.* No staurolite is formed in the rock at a further decrease in the CaO content.

Effect of the bulk-rock MgO concentration on staurolite stability (Fig. 3d). At P = 26.6 kbar, T = 660°C, and the unmodified composition of the rock, it is made up of a mineral assemblage that is dominated by garnet and zoisite (in vol %): *St* 2.25, *Grt* 53.22, *Zo* 29.15, *Cpx* 8.15, *Ms* 3.95, *Rt* 0.38, *Bt* 2.90. The garnet is dominated by grossular and contains lower concentrations of almandine and pyrope. The staurolite is magnesian: $X_{\mathrm{Mg}\text{-}St}$ = 0.69. The clinopyroxene is jadeite.

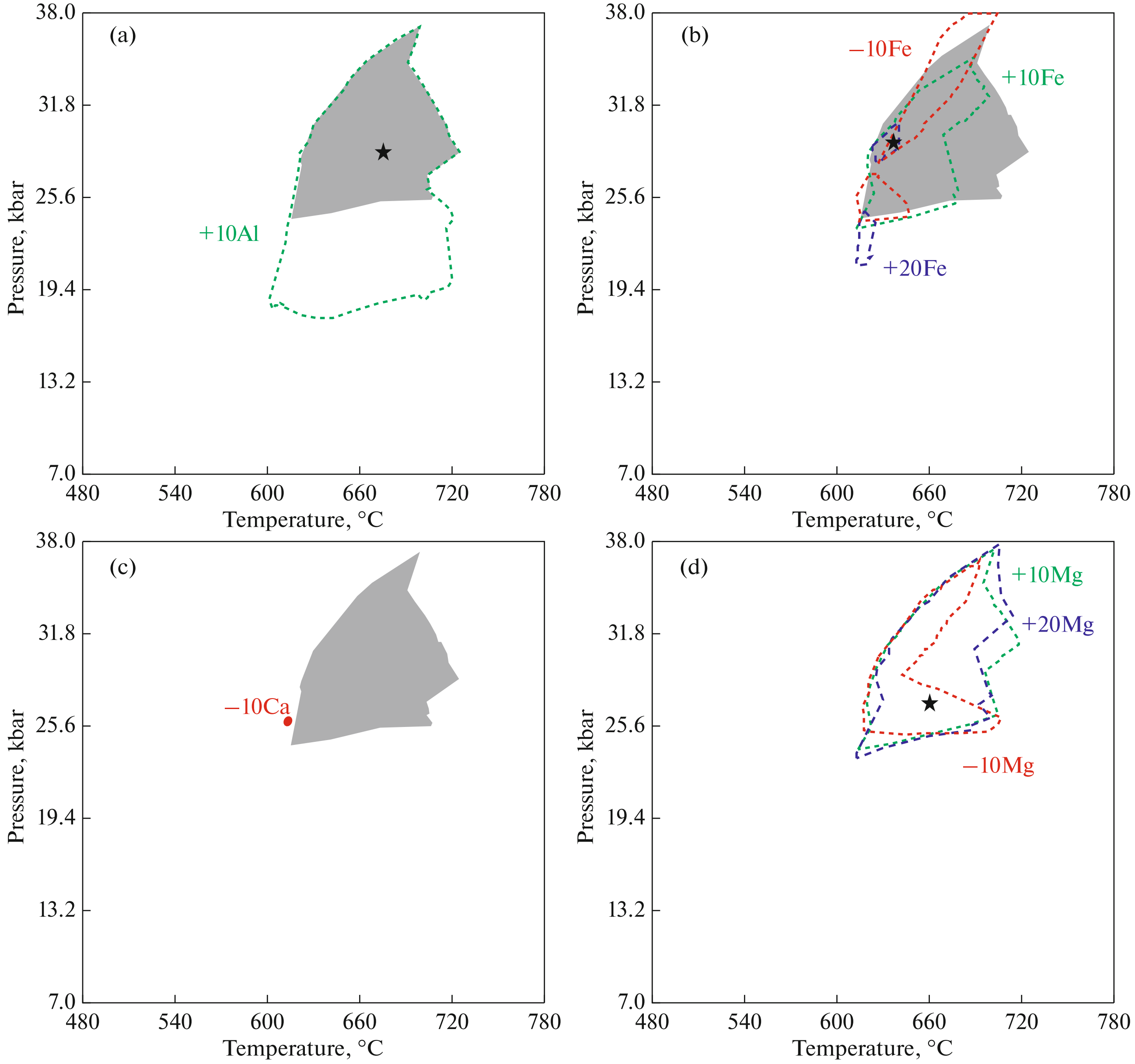

Fig. 3. Changes in the configurations of staurolite stability fields in P–T diagrams with variations in the concentrations of major components in the protolith. The basic composition of the metabasite was assumed to be that of sample LMG. (a) Al_2O_3, (b) FeO_t, (c) CaO, (d) MgO. Other symbols are as in Fig. 2.

An increase in the MgO content by 10% leads to a small increase in the amount of staurolite to 3.7 vol %, a decrease in the biotite content, and the disappearance of muscovite. The composition of the minerals practically does not change. An increase in the MgO content by 20% relative to the unmodified composition results in an insignificant increase in the staurolite content, the crystallization of amphibole, and in that the clinopyroxene enriches in the jadeite component.

Sample Lm-185. For the composition of the metabasite of sample Lm-185, staurolite-bearing mineral assemblages were modeled at P = 25–32 kbar, T = 610–680°C. At P = 26 kbar, T = 630°C (which roughly corresponds to the central part of the staurolite-bearing region), and the rock consists of (in vol %) *St* (2.3) + *Grt* (63.3) + *Cpx* (18.5) + *Ms* (12.2) + *Ky* (2.5) + *Rt* (<1) (Figs. 4a–4d).

Effect of the bulk-rock Al_2O_3 concentration on staurolite stability (Fig. 4a). At P = 28.0 kbar, T = 640°C, and the unmodified composition of the rock, it consists mostly of garnet, clinopyroxene, and muscovite and contains lower concentrations of staurolite, kyanite, and rutile (in vol %): *St* 1.04, *Grt* 65.38, *Cpx* 17.47, *Ms* 12.24, *Ky* 3.17, *Rt* 0.69. The staurolite is

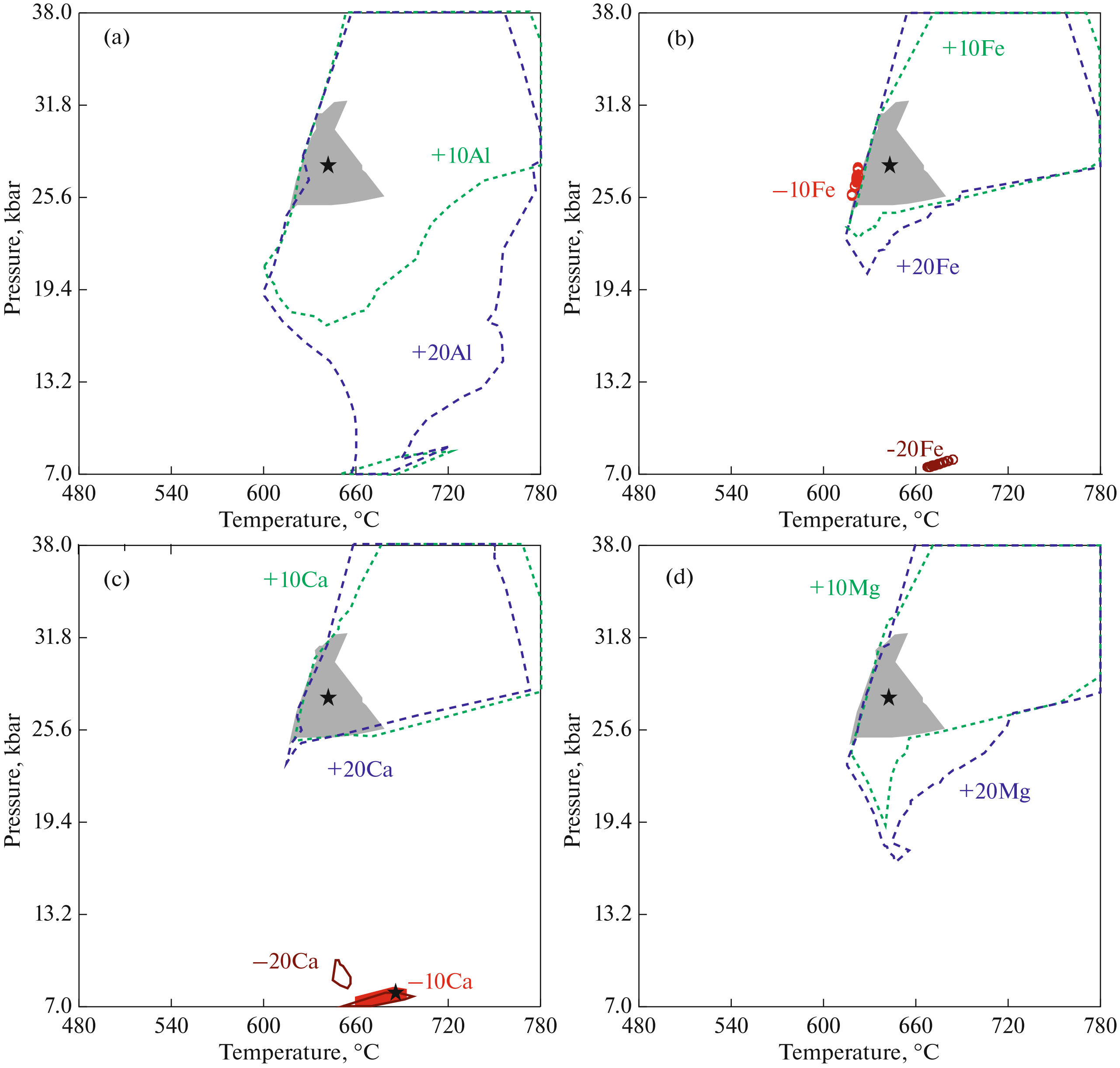

Fig. 4. Changes in the configurations of staurolite stability fields in *P–T* diagrams with variations in the concentrations of major components in the protolith. The basic composition of the metabasite was assumed to be that of sample Lm-185. (a) Al_2O_3, (b) FeO_t, (c) CaO, (d) MgO. Other symbols are as in Fig. 2.

mostly magnesian ($X_{Mg\text{-}St}$ = 0.76), and the garnet is dominantly pyrope and contains approximately equal concentrations of the grossular and almandine components: $Prp_{0.42}Grs_{0.30}Alm_{0.28}Sps_{0.008}$. The clinopyroxene has the composition $X_{Di} = 0.06$, $X_{Jd} = 0.19$, $X_{Hed} = 0.008$, $X_{Om} = 0.67$. The mica consists mostly of muscovite: $X_{Ms} = 0.65$, $X_{Pg} = 0.33$, $X_{Cel} = 0.23$.

An increase in the Al_2O_3 content by 10% significantly increases the amount of staurolite in the rock and leads to the crystallization of biotite and instability of kyanite (in vol %): *St* 13.92, *Grt* 57.64, *Cpx* 16.08, *Bt* 8.17, *Ms* 3.68, *Rt* 0.51. The garnet becomes thereby less magnesian ($Prp_{0.34}Grs_{0.35}Alm_{0.30}Sps_{0.009}$), as also does the staurolite ($X_{Mg\text{-}St}$ = 0.74). A further increase in the alumina content by 20% leads to an increase in the staurolite content in the rock, a drastic decrease in the omphacite content because of the development of amphibole, and the disappearance of muscovite (in vol %): *St* 17.37, *Grt* 52.19, *Cpx* 4.23, *Amp* 14.41, *Bt* 11.37, *Rt* 0.43. The X_{Mg} of the staurolite and garnet continues to decrease ($Prp_{0.27}Grs_{0.41}Alm_{0.30}Sps_{0.01}$, $X_{Mg\text{-}St}$ =

0.72), and the biotite is mostly magnesian ($X_{Phl} = 0.50$, $X_{Eas} = 0.23$, $X_{Ann} = 0.06$).

A decrease in the Al_2O_3 content by 10% from that in the unmodified composition results in that no staurolite is formed, and instead talc and lawsonite are stable and quartz starts to crystallize (in vol %): *Grt* (49.85) + *Cpx* (18.85) + *Ms* (11.73) + *Lws* (11.0) + *Tlc* (6.39) + *Ky* (0.66) + *Qz* (0.84) + *Rt* (0.67).

An increase in the Al_2O_3 content in the rock generally leads to a significant increase in the staurolite content (from 1 to 17.4 vol %), whereas the contents of garnet and clinopyroxene, conversely, decrease, kyanite ceases to be stable, and biotite becomes stable. A further increase in the Al_2O_3 content results in that muscovite ceases to be stable, but amphibole begins to crystallize. The X_{Mg} of both the staurolite and the garnet decrease: $X_{Mg\text{-}St} = 0.76–0.72$ and *Prp* = 0.42–0.27. A further decrease in the alumina content leads to that no staurolite is formed, any more and quartz is produced, together with lawsonite and talc.

Effect of the bulk-rock FeO$_t$ concentration on staurolite stability (Fig. 4b). At *P* = 28.0 kbar, *T* = 640°C, and the unmodified bulk-rock composition, the rock is dominated by garnet, clinopyroxene, and muscovite and contains subordinate amounts of staurolite, kyanite, and rutile (in vol %): *St* 1.04, *Grt* 65.38, *Cpx* 17.47, *Ms* 12.24, *Ky* 3.17, *Rt* 0.69. The garnet has the composition $Prp_{0.42}Grs_{0.30}Alm_{0.28}Sps_{0.008}$, and the staurolite possesses $X_{Mg\text{-}St} = 0.76$.

An increase in the FeO_t content by 10% leads to a substantial increase in staurolite abundance and to a decrease in the content of muscovite, and to the disappearance of kyanite (in vol %): *St* 5.47, *Grt* 65.37, *Cpx* 16.48, *Ms* 8.87, *Rt* 0.63. The X_{Mg} of the garnet and staurolite decreases: $Prp_{0.38}Grs_{0.31}Alm_{0.30}Sps_{0.008}$, $X_{Mg\text{-}St}$ = 0.74. As the FeO_t content continues to increase, the amount of staurolite increases, those of clinopyroxene and muscovite decrease, and biotite is formed (in vol %): *St* 7.13, *Grt* 64.80, *Cpx* 15.52, *Bt* 8.17, *Ms* 3.83, *Rt* 0.56. The X_{Mg} of the garnet and staurolite continues to decrease: $Prp_{0.35}Grs_{0.32}Alm_{0.32}Sps_{0.008}$, $X_{Mg\text{-}St}$ = 0.73. The biotite is dominated by the phlogopite end member: $X_{Phl} = 0.59$, $X_{Eas} = 0.14$, $X_{Ann} = 0.05$, $X_{Ti\text{-}Bt} = 0.09$.

An increase in FeO_t content in the rock thus leads to an increase in staurolite content (from 1 to 7 vol %), a decrease in the contents of muscovite, and the disappearance of kyanite. The X_{Mg} of the staurolite and garnet may also slightly decrease. A significant increase in the FeO_t content leads to the crystallization of biotite, and a decrease in the FeO_t content significantly diminishes the fields of staurolite-bearing mineral assemblages and leads to the crystallization of amphibole, plagioclase, and quartz.

Effect of the bulk-rock CaO concentration on staurolite stability (Fig. 4c). At *P* = 28.0 kbar, *T* = 640°C, and the unmodified rock composition, this rock is dominated by garnet, clinopyroxene, and muscovite and contains smaller amounts of staurolite, kyanite, and rutile (in vol %): *St* 1.04, *Grt* 65.38, *Cpx* 17.47, *Ms* 12.24, *Ky* 3.17, *Rt* 0.69. The composition of the garnet is $Prp_{0.42}Grs_{0.30}Alm_{0.28}Sps_{0.008}$, and the equilibrium staurolite has $X_{Mg\text{-}St} = 0.76$.

An increase in the CaO content by 10% increases the content of staurolite and leads to that kyanite ceases to be stable but biotite crystallizes (in vol %): *St* 6.11, *Grt* 64.30, *Cpx* 16.98, *Ms* 7.73, *Bt* 4.27, *Rt* 0.61. The garnet therewith is depleted in pyrope, $Prp_{0.37}Grs_{0.35}Alm_{0.28}Sps_{0.008}$, and the composition of the staurolite does not change: $X_{Mg\text{-}St}$ = 0.76. A further increase in the CaO content by 20% slightly increases the amount of staurolite in the rock and leads to the disappearance of muscovite and to the appearance of zoisite (in vol %): *St* 7.79, *Grt* 61.22, *Cpx* 16.13, *Bt* 11.75, *Zo* 2.60, *Rt* 0.50. The garnet becomes less magnesian, as also does the staurolite: $Prp_{0.32}Grs_{0.39}Alm_{0.28}Sps_{0.009}$ and $X_{Mg\text{-}St}$ = 0.74, respectively.

An increase in the CaO content thus expands the stability region of staurolite-bearing mineral assemblages and increases the amount of staurolite from 1 to 7.8 vol % and results in that kyanite and biotite cease to be stable and that zoisite becomes stable. The staurolite becomes less magnesian, and the garnet becomes depleted in the pyrope end member at an increase in the grossular concentration. A decrease in the CaO content does not lead to changes in the stability region of staurolite-bearing mineral assemblages at low pressures, under which assemblages are stable that are dominated by amphibole and plagioclase (anorthite) and contain subordinate amounts of garnet. Staurolite in the low-pressure region is notably less magnesian: $X_{Mg\text{-}St} = 0.46$.

Effect of the bulk-rock MgO concentration on staurolite stability (Fig. 4d). At *P* = 28.0 kbar, *T* = 640°C, and the unmodified rock composition, the rock consists mostly of garnet, clinopyroxene, and muscovite and contains lower concentrations of staurolite, kyanite, and rutile (in vol %): *St* 1.04, *Grt* 65.38, *Cpx* 17.47, *Ms* 12.24, *Ky* 3.17, *Rt* 0.69. The garnet has the composition $Prp_{0.42}Grs_{0.30}Alm_{0.28}Sps_{0.008}$, and the staurolite has $X_{Mg\text{-}St} = 0.76$.

An increase in the bulk-rock MgO concentration by 10% increases the content of staurolite in the rock, and therewith kyanite disappears and biotite appears (in vol %): *St* 6.76, *Grt* 63.42, *Cpx* 17.29, *Ms* 6.41, *Bt* 5.53, *Rt* 0.58. The garnet slightly depletes in pyrope, and the compositions of all other minerals practically do not change. An increase in the MgO content by 20% relative to the unmodified rock composition leads to that muscovite ceases to be stable and chloritoid crystallizes (in vol %): *St* 5.02, *Grt* 60.84, *Cpx* 16.38, *Ctd* 5.57, *Bt* 11.66, *Rt* 0.53. Because the rock is highly magnesian, the chloritoid has $X_{Mg\text{-}Ctd} = 0.86$, although the garnet slightly depletes in the pyrope component: $Prp_{0.38}Grs_{0.33}Alm_{0.28}Sps_{0.009}$. The staurolite becomes slightly more magnesian: $X_{\mathrm{Mg}\text{-}St} = 0.77$. The biotite is magnesian: $X_{Phl} = 0.64$, $X_{Eas} = 0.13$, $X_{Ann} = 0.04$, $X_{\mathrm{Ti}\text{-}Bt} = 0.09$. A decrease in the bulk-rock MgO content by 10% results in that no staurolite is formed, but lawsonite and talc become stable.

An increase in the MgO content in the rock thus increases the staurolite content (from 1 to 5–6 vol %), kyanite becomes unstable, biotite starts to crystallize, and what is important, magnesian chloritoid becomes stable (to 5.6 vol %). Pyrope concentration in the garnet decreases, and the composition of the staurolite practically does not change. If MgO content in the rock decreases, no staurolite is formed at all.

Mineral Assemblages, Crystallization Sequences of Minerals, and Systematic Variations in the X_{Mg} of the Minerals

The general features of the mineral assemblages and their systematic variations with temperature and pressure variations are described in much detail below with reference to amphibolite with roughly equal Fe and Mg contents (sample Lm-185, Fig. 5a–5c). The changes in the mineral assemblages are discussed for the P–T field passing across the region with staurolite-bearing assemblages (Fig. 5b). For this pseudosection, staurolite is modeled to become stable after such Fe–Mg minerals as chlorite and amphibole become unstable. Talc becomes unstable slightly before, and kyanite appears in the rock in a while. Therewith the staurolite-bearing assemblage contains much garnet and muscovite (Fig. 5b).

Note that the X_{Mg} of the staurolite is higher than that of the garnet (Fig. 5c), which is consistent with the aforementioned data that this is indeed the case under high pressures (Koch-Müller, 1997). The X_{Mg} of the staurolite is weakly negatively correlated with these parameters of the clinopyroxene and garnet and with the concentration of the celadonite end member in the muscovite (Fig. 5c).

The discussed example demonstrates that an elevated X_{Mg} of staurolite in amphibolites is inherited from the high X_{Mg} of minerals whose decomposition gave rise to the staurolite.

Estimation of the Effect of the Metamorphic Fluid Composition on the Stability of Staurolite-Bearing Mineral Assemblages

To estimate how the mineral assemblages depend on the fluid composition, we have simulated the mineral-forming processes at various H_2O and CO_2 proportions in the fluid. The composition of the fluid varied from pure H_2O to almost pure CO_2 by adding CO_2 at $X_{\mathrm{CO_2}}$ increments of 0.2 ($X_{\mathrm{CO_2}}$ = 0–0.8). The changes were simulated for the compositions of metabasite samples 80 (Gil Ibarguchi et al., 1991), LMG (Tsujimori and Liou, 2004), and Lm-185 (Faryad and Hoinkes, 2006), all of which are rich in alumina but differ from one another in the Fe/Mg ratio, which turned out to be critical for staurolite stability.

For sample 80, mineral assemblages stable in the presence of pure H_2O fluid were characterized above (Fig. 2). An increase in the $X_{\mathrm{CO_2}}$ to 0.8 significantly expands the stability fields of staurolite-bearing assemblages and shifts them toward lower temperatures and pressures (Fig. 6a). For example, an increase in $X_{\mathrm{CO_2}}$ by 0.2 results in a shift of the staurolite-bearing region by 20–30°C and ~1 kbar. Also, it is worth mentioning that the high- and medium-pressure regions merge into a single one at $X_{\mathrm{CO_2}} = 0.6$, this region maximally expands at $X_{\mathrm{CO_2}} = 0.2$ in the range of P = 7.6–30 kbar, T = 530–630°C, and this is not accompanied by any qualitative changes in the mineral assemblages.

For the amphibolite of sample LMG, for which a broad P–T region of staurolite-bearing mineral assemblages was modeled in the presence of H_2O fluid (Fig. 6b), an increase in $X_{\mathrm{CO_2}}$ significantly shifts the stability region of staurolite-bearing assemblages toward lower temperatures and expands it along the pressure axis. At $X_{\mathrm{CO_2}} = 0.8$, staurolite is stable at P = 20–41 kbar, T = 520–610°C, but its temperature stability range dramatically shrinks at P = 23–26 kbar, T = 540–560°C. No qualitative changes in the mineral assemblages have been found.

Sample Lm-185 shows a significant difference between the stability regions of staurolite-bearing mineral assemblages in the presence of pure H_2O and H_2O–CO_2 fluids (Fig. 6c). At $X_{\mathrm{CO_2}} = 0.2$, the stability region of staurolite-bearing mineral assemblages shifts for ~1.5 kbar toward higher pressures and for ~20°C toward lower temperatures. At $X_{\mathrm{CO_2}} = 0.4$, the high-pressure region shrinks and is shifted toward higher pressures and lower temperatures. Therewith a small region appears at low pressures, at P = 6–6.5 kbar, T = 620–635°C, in which staurolite assemblages with amphibole, plagioclase, and quartz occur. At $X_{\mathrm{CO_2}}$ = 0.6, the high-pressure staurolite-bearing region significantly shrinks and is shifted toward higher pressure and lower temperature: P = 32–34 kbar, T = 580–600°C. The low-pressure region, conversely, expands and is shifted toward lower pressures and temperatures. At $X_{\mathrm{CO_2}} = 0.8$, only the low-pressure region remains, which expands and is shifted toward lower temperature: P = 4.5–8 kbar, T = 500–530°C.

An increase in $X_{\mathrm{CO_2}}$ in the H_2O–CO_2 fluid systematically shifts the stability region of staurolite-bearing mineral assemblages toward lower temperatures. For some of the metabasite samples (samples 80 and LMG), an increase in $X_{\mathrm{CO_2}}$ expands the stability field

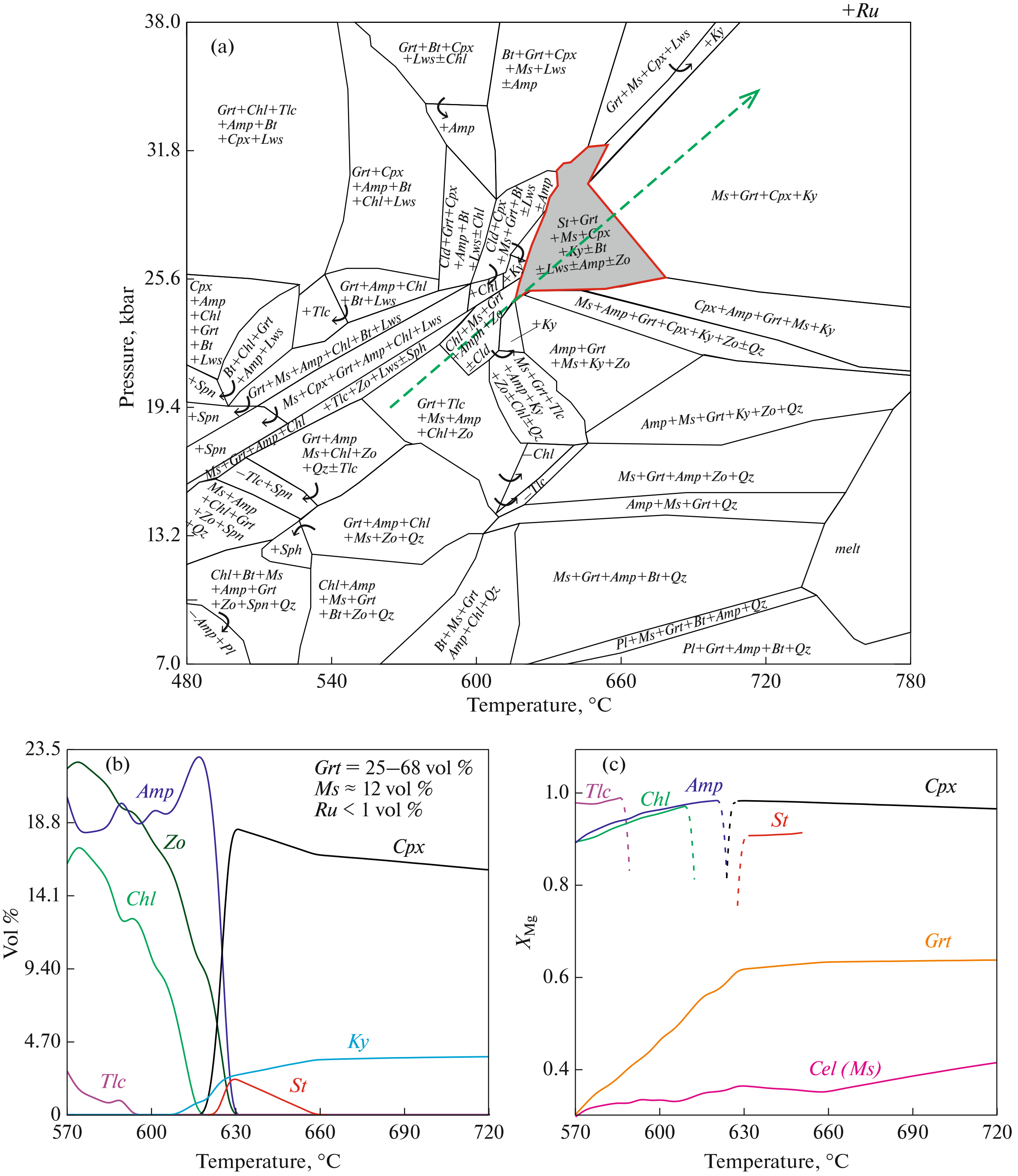

Fig. 5. Diagrams showing mineral assemblages, crystallization sequences, and variations in X_{Mg} of minerals for the specified *P*–*T* ranges and paths. (a) *P*–*T* diagram (pseudosection) of the stability fields of mineral assemblages for the composition of Lm-185. The red contour outlines the staurolite field. The signs “+” and “–” indicate that the specified mineral phase is present or absent, respectively, in the field indicated by an arrow. The green dashed line with an arrowhead is the *P*–*T* path along which the changes in the contents of minerals and their X_{Mg} are analyzed (Figs. 5b, 5c); (b) content (vol %) of minerals for the specified *P*–*T* path; (c) variations in the X_{Mg} of the Fe–Mg silicates along the *P*–*T* path.

of staurolite assemblages along both the temperature and the pressure axes, whereas this high-pressure region of sample Lm-185, conversely, decreases and is shifted far up the pressure axis. A low-pressure field in which staurolite assemblages with amphibole, plagioclase, and quartz are stable appears only starting at $X_{CO_2} = 0.4$, and a further increase in X_{CO_2} in the fluid expands this field.

The aforementioned changes in the configuration of the stability fields with variations in X_{CO_2} in the fluid can be explained by changes in the H_2O activity, whose decrease with increasing X_{CO_2} diminishes the temperature stability of hydrous minerals, instead of which relatively less hydrous minerals are formed, for example, staurolite.

Effect of the Fe^{3+}/Fe^{2+} Ratio of the Rock on Staurolite Stability

Earlier simulations of the mineral-forming processes have convincingly demonstrated (White et al., 2000) that staurolite stability should be necessarily analyzed with regard to the average Fe^{3+} concentration in the rock. Although it is hard to reasonably accurately and confidently evaluate the Fe^{3+}/Fe^{2+} ratio of rocks when the mineral-forming processes proceeded in them, if can be assumed that the Fe_2O_3/FeO ratio of the basites was 0.15 (Brooks, 1976) or 0.20–0.25 (Hughes and Hussey, 1979), and this leads to a slight expansion of the staurolite stability field in these rocks than in compositions with $FeO_t = FeO$. However, bearing in mind that the thermodynamic data on Fe^{3+}-bearing silicates are still sparse, one has to be cautious with such evaluations, and hence, herein we do not included Fe^{3+} in our simulations.

DISCUSSION AND DETERMINING THE PETROCHEMICAL MODULI

The broad diversity of naturally occurring mineral assemblages of metabasites suggests that the number of phases and their relationships strongly depend on the *P*–*T* parameters, bulk-rock compositions, and the composition of the fluids (Figs. 6a–6c, 7). Alumina content in the rocks is crucial for the stability of hornblende and staurolite. This conclusion is consistent with data in (Arnold et al., 2000) that staurolite and hornblende are formed in rocks with $Al_2O_3/(Al_2O_3 +$

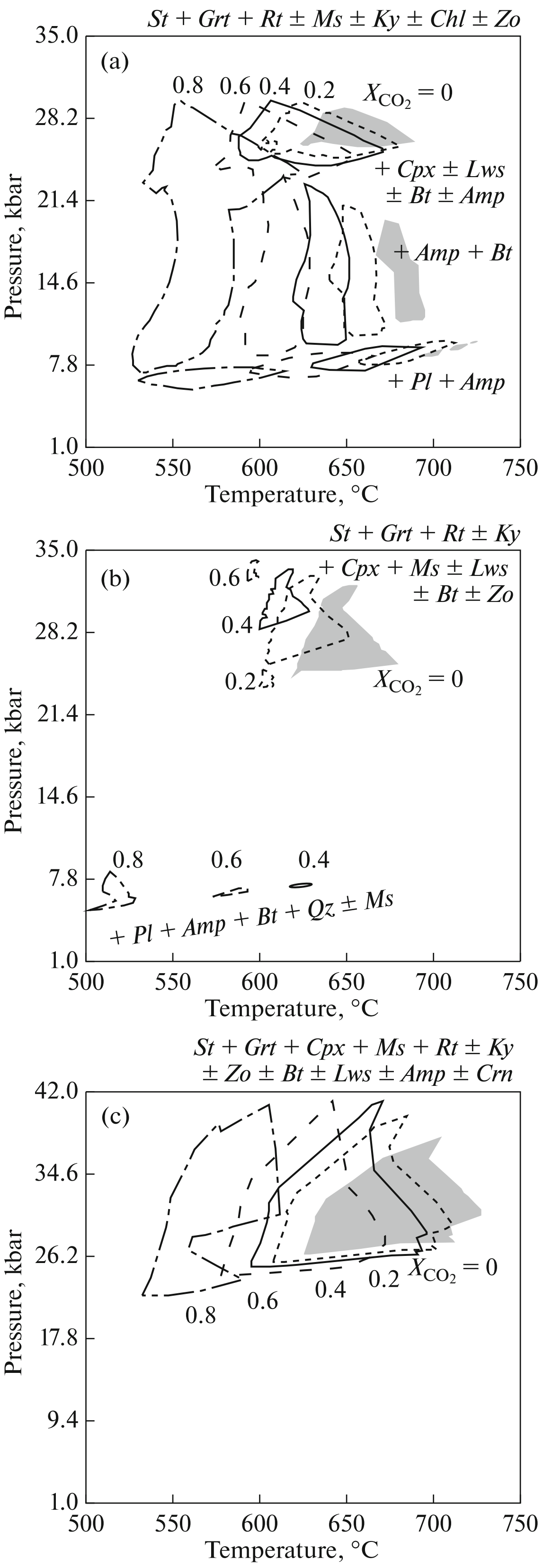

Fig. 6. Changes in the configurations of the stability fields of staurolite-bearing mineral assemblages depending on the fraction of CO_2 in the H_2O–CO_2 fluid. Gray fields are the stability fields of staurolite in the presence of pure H_2O fluid. Various lines show variations in X_{CO_2} of the fluid, from 0.2 to 0.8. (a) Modeling for the composition of sample 80, (b) same for sample Lm-185, (c) same for sample LMG.

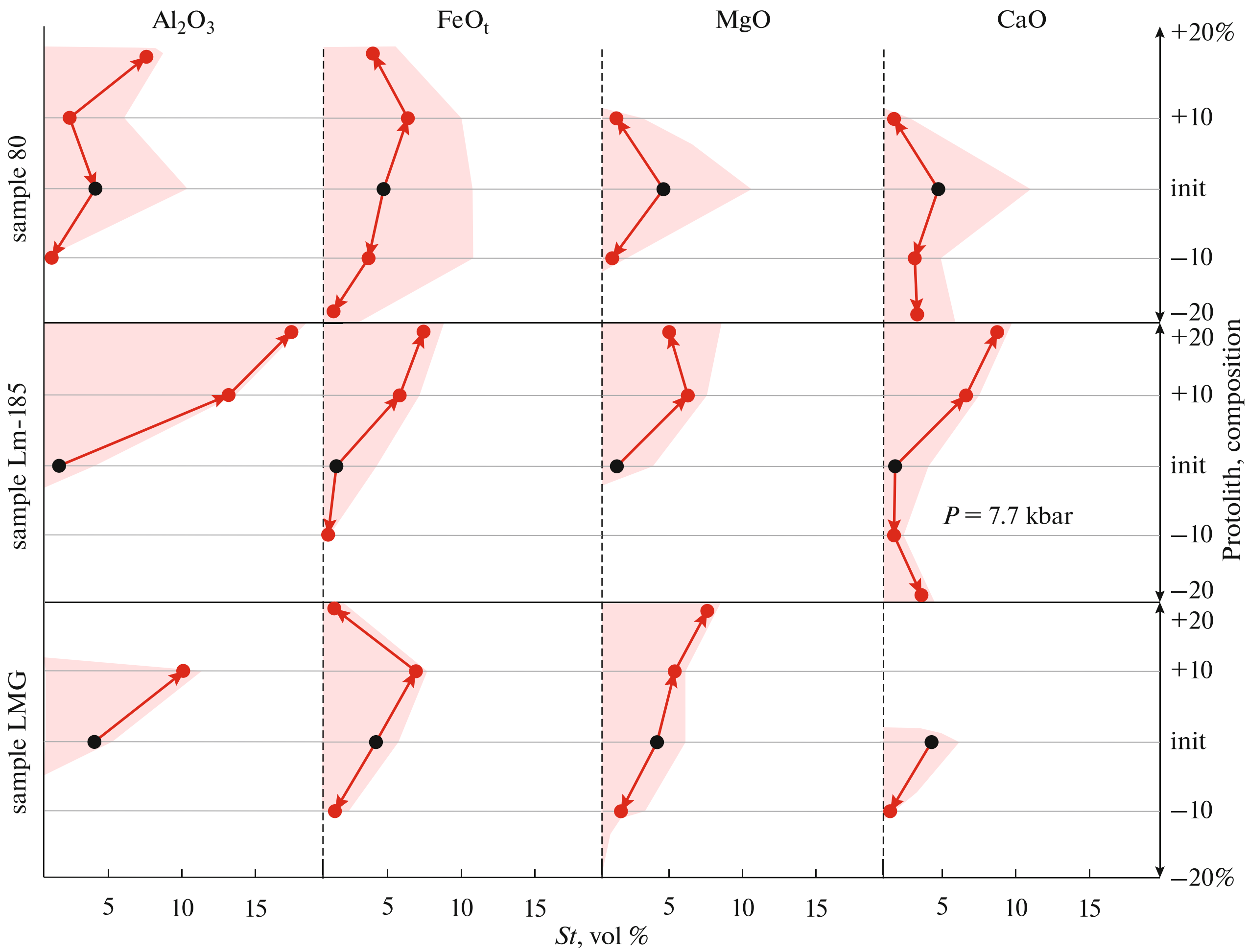

Fig. 7. Variations in the content (vol %) of staurolite depending on concentrations of major components (Al_2O_3, FeO_t, MgO, and CaO) at their changes at increments of ±10 and ±20% for the various unmodified compositions of the protolith.

FeO + MgO + CaO + Na_2O) = 35 wt % at temperatures above 550°C and 595°C, respectively. The X_{Mg} of the staurolite lies within the range of 0.2 to 0.7. Thermodynamic simulations with the THERMOCALC software (Powell and Holland, 1988) indicate that staurolite- and hornblende-bearing mineral assemblages can be formed at pressures of 4–10 kbar and temperatures of 560–650°C. In such rocks (except Al- and Fe-richer lithologies), staurolite assemblages are stable within a narrow *P–T* field (Arnold et al., 2000). Analogously, according to (Tsujimori and Liou, 2004), the assemblage *Hbl* + *Czo* + *Ky* ± *St* + *Pg* + *Ab* ± *Crn* in Al-rich metabasites is typical of metamorphic parameters of the high-pressure epidote-amphibolite facies.

Although the occurrence of staurolite in “typical” amphibolites may be indicative of metamorphism under a relatively high pressure, interpretations of these assemblages in more aluminous lithologies are more ambiguous. Because of the high variability of staurolite-bearing mineral assemblages, the crystallization sequences of the minerals during metamorphism are uncertain (Arnold et al., 2000; Faryad and Hoinkes, 2006).

It is difficult to anticipate the stability of staurolite in the mineral assemblages of metabasites because this mineral is rarely documented in such rocks. One of the reasons for this is (Purtscheller and Mogessie, 1984) that it is difficult to identify staurolite phases in metabasites because their grains are small.

Although staurolite and kyanite are found in amphibolite-facies rocks and usually occur in association with paragonite and garnet, amphibole may be absent from some Al-rich metabasites (Faryad and Hoinkes, 2006). Staurolite was also documented in metabasites containing gedrite (Spear, 1977, 1978, 1980).

The aforementioned facts and considerations imply that staurolite-forming reactions in metabasites are controlled by several factors in addition to alumina content. Staurolite and kyanite stability in rocks strongly depends on their Fe and Mg concentrations (Arnold et al., 2000; Faryad and Hoinkes, 2006).

Sometimes an important role is played by K_2O. Low K_2O concentrations hamper the formation of potassic feldspar, and hence, excess Al (if present), is accommodated to some extent in plagioclase and is favorable for staurolite stability in the presence of relatively high Fe concentrations.

Data in (Faryad and Hoinkes, 2006) show that staurolite can be formed in high-Al metabasites at $T = 570°C$, $P > 10$ kbar, together with clinozoisite, or at $T = 540–450°C$, $P = 7–8$ kbar, with plagioclase. The absence of chloritoid from the studied rock samples suggests either that this mineral has been completely replaced or that the prograde $P–T$ path did not cross the stability field of chloritoid (Faryad and Hoinkes, 2006).

Metabasites typically contain staurolite that is more magnesian than it is in metapelites. Staurolite in which much Fe^{2+} is substituted for Mg was first found in high-pressure metamorphic rocks in the 1980s (Schreyer et al., 1984). Later on, magnesian staurolite has been found in other metabasites (e.g., Enami and Zang, 1988; Gil Ibarguchi et al., 1991). One of the first studied magnesian staurolite ($X_{Mg} = 0.965$) samples originated from the Dora-Maira massif in the western Alps (Simon et al., 1997; Simon and Chopin, 2001) and contained much H^+. This staurolite was reportedly formed under ultrahigh-pressure metamorphism at $T = 700°C$ and $P = 30$ kbar (Simon et al., 1997; Simon and Chopin, 2001).

Staurolite samples with X_{Mg} up to ~0.4–0.6 were found in various rocks metamorphosed under high pressures (Schreyer et al., 1984; Ward, 1984, Grew and Sandiford, 1984; Nicollet, 1986). Magnesian staurolite is often found in equilibrium coexistence with corundum. This indicates that an environment undersaturated with silica is favorable for the origin of highly magnesian staurolite (e.g., Schreyer, 1967; Grew and Sandiford, 1985). However, it is important to recall that these finds of highly magnesian staurolite were made in metapelites of unusual composition, undersaturated with K_2O (Korikovsky, 1979), whose other stable phases are amphibole of the gedrite–anthophyllite series, Al_2SiO_5 polymorphs, cordierite, garnet, orthopyroxene, and some other minerals. It has been found that the X_{Mg} of staurolite depends nonlinearly on pressure (see below). It should be kept in mind that detailed studies of staurolite have revealed that the isomorphous exchange of Fe in this mineral can proceed not only for Mg but also for Co, Zn, Mn, and perhaps, also Ca (Fed'kin, 1975). It is still not possible to elucidate how this isomorphic exchange can affect staurolite stability because the properties of such staurolites are still explored very poorly.

It has been hypothesized (Schreyer, 1967) that the absence of natural magnesian staurolite from the upper mantle, in which $P–T$ parameters are reached that are necessary for the stability of magnesian staurolite (>11 kbar), is explained by the absence of highly aluminous rocks. W. Shreyer has also suggested that magnesian staurolite and quartz cannot be stable with each other because of the alternative stability of kyanite or other magnesian silicates. Indeed, kyanite and other aluminous minerals are typical of high-pressure eclogites (e.g., Dawson, 1980), and the breakdown of these minerals at a temperature decrease may result in Mg-rich staurolite.

When the possible sources of highly aluminous rocks at mantle depths were discussed, it was suggested that staurolite can be produced by high-pressure metamorphism in mafic rocks with minor amounts of crustal material, which is characterized by high alumina contents (Hellman and Green, 1979).

It has been experimentally proven (Hellman and Green, 1979) that staurolite can be formed in a mafic rock under a high pressure, in the presence of water. Experiments aimed at constraining the stability field of staurolite in the $MgO–Al_2O_3–SiO_2–H_2O$ system (Fockenberg, 1995) under various water pressure have demonstrated that the mineral is stable at $P = 12–66$ kbar and $T = 608–918°C$. Hydrogen concentration in magnesian staurolite usually increases with increasing pressure (Holdaway et al., 1995; Fockenberg, 1995).

Scarce data are currently available that magnesian staurolite can be formed at very high temperatures (> 900–1000°C), as in the Central Zone of the Limpopo complex in South Africa (Schreyer et al., 1984; Tsunogae and Van Reenen, 2010), where magnesian ($X_{Mg} = 0.44–0.58$) staurolite was found in an equilibrium assemblage with sapphirine and quartz. Another find was made in southern India (Tsunogae and Santosh, 2003; Santosh et al., 2004; Shimpo et al., 2006), where magnesian ($X_{Mg} \sim 0.58$) accessory staurolite was found out to coexist with garnet, gedrite, sapphirine, corundum, spinel, and rutile.

Staurolite can have $X_{Mg} < 0.3$, which is lower than this parameter of other silicates coexisting with it (e.g., Deer et al., 1982; Enami, 1988). However, it is well known that $K_D^{Fe\text{-}Mg}$ of staurolite with, for example, garnet shows an inversion with increasing pressure (Koch-Müller, 1997). Staurolite-bearing K-poor rocks (without muscovite and potassic feldspar) sometimes contain unusual mineral assemblages with gedrite and cordierite, and the staurolite and garnet have the highest X_{Mg}, much higher than these parameters of the minerals in the surrounding muscovite-bearing metapelites metamorphosed to the same temperature and pressure. It is also known (from data on natural rocks) that the reactions forming and decomposing staurolite at prograde metamorphism are principally different: cordierite rims around staurolite have been found and documented in (Mezger and Passchier, 2003).

Table 2. Petrochemical moduli for metabasite groups differing in the FeO/MgO ratio

Metabasites	FeO/MgO	MgO/CaO	CaO/FM*	Al_2O_3/FM	
Group 1	⩾1	0.33	1.11	2.07	max
		0.29	0.97	1.77	min
Group 2	~1	1.21	0.52	1.37	max
		0.97	0.45	1.23	min
Group 3	⩽1	1.31	0.67	1.22	max
		1.11	0.58	1.21	min

* FM = FeO_t + MgO.

Magnesian staurolite has been synthesized at T = 700–950°C and $P > 11$ kbar (Schreyer, 1967; Schreyer and Seifert, 1969). Staurolite rich in Mg (X_{Mg} = 0.53–0.57) was experimentally synthesized from olivine tholeiite at T = 740–760°C and P = 24–26 kbar (Hellman and Green, 1979).

These and other experimental data suggest that Mg-rich staurolite can be stable in Mg- and Al-rich metamorphic rocks produced at high temperatures and pressures, which is consistent with our simulation results.

It follows that the metabasite compositions favorable for staurolite stability in them can be most comprehensively characterized by their Al_2O_3, MgO, FeO_t, and CaO concentrations, and because the concentrations of other major components are lower than or close to unity, variations in the concentrations of these components practically do not affect staurolite stability. With regard to this, the following ratios were assumed as the petrochemical moduli that primarily control staurolite stability: MgO/CaO, CaO/FM, and Al_2O_3/FM. With regard to some features of the stability fields of staurolite in protoliths with various FeO_t contents, these moduli were calculated separately for three compositional groups of the metabasites with contrastingly different FeO/MgO ratios (Table 2, Fig. 8).

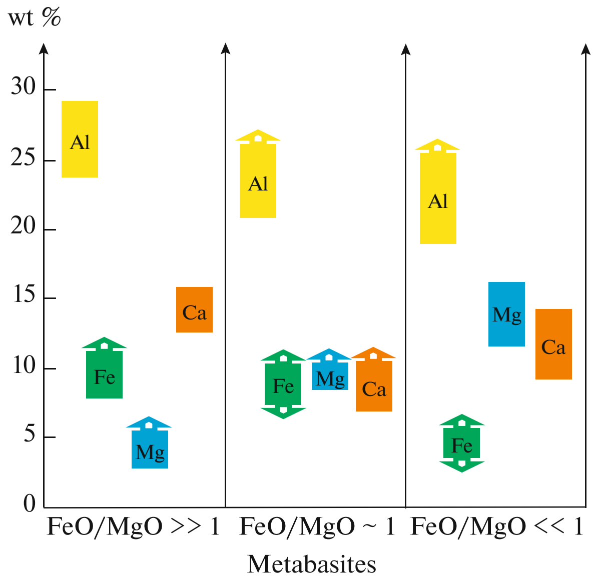

Fig. 8. Ranges of concentrations of major components (Al_2O_3, FeO_t, MgO, and CaO) in mafic protoliths in which staurolite is expected to be formed by metamorphism.

The petrochemical moduli can be utilized to provisionally predict whether staurolite can be stable in metamorphic rocks formed at intermediate and high pressures after certain protoliths.

CONCLUSIONS

The wide variety of mineral assemblages with staurolite in metabasites indicates that the stability of staurolite-bearing assemblages is controlled by several factors: *P*–*T* parameters of metamorphism, bulk-rock compositions of the protoliths, and the composition of the fluids. To better understand the origin of staurolite in the group of metabasites, we classified these rocks into subgroups with different contents of Fe, Mg, Ca, and Al, because ratios of these elements differently affect the configuration and number of *P*–*T* fields of staurolite mineral assemblages. This feature is inherent to metabasites but not metapelites.

The key factors and conditions of staurolite stability are as follows:

1. Staurolite is most typical of metabasites metamorphosed under medium and high pressures.

2. Alumina content in metabasites is of paramount importance for the stability of staurolite-bearing mineral assemblages and directly controls the configuration of the stability field(s) in *P*–*T* space.

3. An increase in the FeO_t content in the rocks decreases the X_{Mg} of the staurolite, and a significant decrease in the FeO_t content results in that amphibole and/or biotite are formed instead of staurolite.

4. A change in the CaO content notably affects the configuration of the staurolite fields: a moderate increase in the CaO content expands the staurolite-bearing region toward higher pressures. However the rock contains a significant highest CaO content, no staurolite is formed. An increase in the CaO content is

associated with a decrease in the X_{Mg} of the staurolite, which is usually controlled by the dominance of amphibole and/or clinopyroxene or sometimes also biotite, which are more magnesian than staurolite. A decrease in the CaO content is less important for staurolite stability: assemblages of this mineral with amphibole and plagioclase with subordinate amounts of garnet are formed at low pressures.

5. The role of MgO content in metabasites is that a decrease in the content of this component drastically decreases the content of staurolite in the rock and simultaneously decreases its X_{Mg}.

6. An increase in the CO_2 mole fraction in the H_2O-CO_2 fluid shifts the stability fields of staurolite assemblages toward lower temperatures and higher pressures in the $P-T$ diagrams.

ACKNOWLEDGMENTS

The authors thank the reviewers I.I. Likhanov and K.A. Savko for the careful reviews of the manuscript and recommendations that led us to improve and append it.

FUNDING

This study was carried out under a government-financed research project for the Institute of Precambrian Geology and Geochronology, Russian Academy of Sciences and was supported by Grant FMUW-2022-0002 from the Ministry of Science and Education of the Russian Federation.

CONFLICT OF INTEREST

The authors declare that they have no conflicts of interest.

REFERENCES

Arnold, J., Powell, R., and Sandiford, M., Ampibolites with staurolite and other aluminous minerals: calculated mineral equilibria in NCFMASH, *J. Metamorph. Geol.,* 2000, vol. 18, no. 1, pp. 23–40.

Borisova, E.B. and Baltybaev, Sh.K., Petrochemical criteria of staurolite stability in metapelites at medium-temperature low- and medium-pressure metamorphism, *Petrology,* 2021, vol. 29, no. 4, pp. 336–350.

Brooks, C.K., The Fe_2O_3/FeO ratio of basaltic analyses: an appeal for a standardized procedure, *Bull. Geol. Soc. Denmark,* 1976, vol. 25, pp. 117–120.

Connolly, J.A., Multivariable phase-diagrams - an algorithm based on generalized thermodynamics, *Am. J. Sci.,* 1990, vol. 290, pp. 666–718.

Dawson, J.B., *Kimberlites and their Xenoliths,* Berlin–Heidelberg: Springer-Verlag, 1980.

Deer, W.A., Howie, R.A., and Zussman, J., *Rock-Forming Minerals. Vol. 1a: Orthosilicates,* New York: Halsted Press, 1982.

Enami, M. and Zang, Q., Magnesian staurolite in garnet-corundum rocks and eclogite from the Donghoi District, Jiangsu Province, EAS China, *Am. Mineral.,* 1988, vol. 73, pp. 48–58.

Faryad, S.W. and Hoinkes, G., Reaction textures in Al-rich metabasite; implication for metamorphic evolution of the eastern border of the Middle Austroalpine basement units, *Lithos,* 2006, vol. 90, pp. 145–157.

Fed'kin, V.V., *Stavrolit. Sostav, svoistva, paragenezisy i usloviya obrazovaniya* (Staurolite: Composition, Properties, Parageneses, and Conditions of Formation), Moscow: Nauka, 1975.

Fockenberg, T., Synthesis and chemical variability of Mg-staurolite in the system $MgO-Al_2O_3-SiO_2-H_2O$ as a function of water pressure, *Eur. J. Mineral.,* 1995, vol. 7, pp. 1373–1380.

Grew, E.S. and Sandiford, M., Staurolite in a garnet–hornblende–biotite schist from the Lanterman Range, northern Victoria Land, Antarctica, *N. Jahrb. Mineral.,* 1985, vol. 9, pp. 396–410.

Hellman, P.L. and Green, T.H., The high-pressure experimental crystallization of staurolite in hydrous marine compositions, *Contrib. Mineral. Petrol.,* 1979, vol. 68, pp. 369–372.

Helms, T.S., McSween, H.Y., Laolka, T.C., and Jarosewich, F.E., Petrology of a Georgia Blue Ridge ampibolite unit with hornblende–gedrite–kyanite–staurolite, *Am. Mineral.,* 1987, vol. 72, pp. 1086–1096.

Holdaway, M.J. and Mukhopadhyay, B., Thermodynamic properties of stoichiometric staurolite $H_2Fe_4Al_{18}Si_8O_{48}$ and $H_6Fe_2Al_{18}Si_8O_{48}$, *Am. Mineral.,* 1995, vol. 80, pp. 520–533.

Holland, T.J.B. and Powell, R., An improved and extended internally consistent thermodynamic dataset for phases of petrological interest, involving a new equation of state for solids, *J. Metamorph. Geol.,* 2011, vol. 29, pp. 333–383.

Hughes, C.J. and Hussey, E.M., Standardized procedure for presenting corrected Fe_2O_3/FeO ratios in analyses of fine-grained mafic rocks, *N. Jb. Mineral. Mh.,* 1979, vol. 12, pp. 570–572.

Humphreys, H.S., Metamorphic evolution of amphibole-bearing aluminous gneisses from the Eastern-Namaqua Province, South Africa, *Am. Mineral.,* 1993, vol. 78, pp. 1041–1055.

Ibarguchi, J.I. and Mendia, M., Mg- andC-rich staurolite and Cr-rich kyanite in high-pressure ultrabasic rocks (Cabo Ortegal, northwestern Spain), *Am. Mineral.,* 1991, vol. 76, pp. 501–511.

Koch-Müller, M., Experimentally determined Fe–Mg exchange between synthetic staurolite and garnet in the system $MgO-FeO-Al_2O_3-SiO_2-H_2O$, *Lithos,* 1997, vol. 41, pp. 185–212.

Korikovsky, S.P., *Fatsii metamorfizma metapelitov* (Metamorphic Facies of Metapelites), Moscow: Nauka, 1979.

Kuhns, R.J., Sawkin, F.J., and Ito, E., Magmatism, metamorphism and deformation at Helmo, Ontario, and the timing of Au–Mo mineralization in the Golden Giant mine, *Econ. Geol. Bull. Soc. Econ. Geol,* 1994, vol. 89, pp. 720–756.

López, V. and Soto, J., Metamorphism of calc-silicate rocks from the Alboran basement, Zahn, R., Comas, M., and Klaus, A., Eds., *Proceedings of the Ocean Drilling Program, Scientific Results,* 1991, vol. 161, pp. 251–259.

Mezger, J.E. and Passchier, C.W., Polymetamorphism and ductile deformation of staurolite-cordierite schist of the

Bossost Dome: indication for Variscan extension in the axial zone of the central Pyrenees, *Geol. Mag.,* 2003, vol. 140, no. 5, pp. 595–612.

Nicollet, C., Saphirine et staurotide riche en magnésium et chrome dans les amphibolites et anorthosites à corindon du Vohibory Sud, Madagascar, *Bull. Mineral.,* 1986, vol. 109, pp. 599–612.

Powell, R., Holland, T.J.B., and Worley, B., Calculating phase diagrams involving solid solutions via non-linear equations, with examples using THERMOCALC, *J. Metamorph. Geol.,* 1998, vol. 16, pp. 577–588.

Purttscheller, F. and Mogessie, A., Staurolite in garnet ampibolite from Solden, Otztal old crystalline basement, Austria, *Tschermaks Mineral. Petrograph. Mitt.,* 1984, vol. 32, pp. 223–233.

Ríos, C.A. and Castellanos, O.M., First report and significance of the staurolite metabasites associated to a sequence of calc-silicate rocks from the Silgara Formation at the Central Santander Massif, Colombia, *Rev. Acad. Colombiana Ciencias Exactas, Fis.Natural.,* 2014, vol. 38, no. 149, pp. 418–429.

Ríos, C.A., Castellanos, O.M., Gómez, S.I., and Avila, G., Petrogenesis of the metacarbonate and related rocks of the Silgara Formation, Central Santander massif, Colombian Andes: an overview of a “reaction calcic exoscarn”, *Earth Sci. Res. J.,* 2008, vol. 12, pp. 72–106.

Santosh, M., Tsunogae, T., and Koshimoto, S., First report of sapphirine-bearing rocks from the Palghat–Cauvery shear zone system, southern India, *Gondwana Res.,* 2004, vol. 7, pp. 620–626.

Schreyer, W., A reconnaissance study of the system MgO–Al_2O_3–SiO_2–H_2O at pressures between 10 and 25 kb, *Year Book – Carnegie Inst. Washington,* 1967, vol. 6, pp. 380–392.

Schreyer, W. and Seifert, F., High-pressure phases in the system MgO–Al_2O_3–SiO_2–H_2O, *Am. J. Sci.,* 1969, vol. 267-A, pp. 407–443.

Schreyer, W., Horrocks, P.C., and Abraham, K., High-magnesium staurolite in a sapphirine-garnet rock from the Limpopo Belt, Southern Africa, *Contrib. Mineral. Petrol.,* 1984, vol. 86, pp. 200–207.

Selverstone, J., Spear, F.S., Franz, G., and Morteani, G., *P-T-t* paths for hornblende + kyanite + staurolite garbenschists: high-pressure metamorphism in the western Tauern Window, Australia, *J. Petrol.,* 1984, vol. 25, pp. 501–531.

Shimpo, M., Tsunogae, T., and Santosh, M., First report of garnet–corundum rocks from Southern India: implications for prograde high-pressure (eclogite-facies?) metamorphism, *Earth Planet. Sci. Lett.,* 2006, vol. 242, pp. 111–129.

Simon, G. and Chopin, C., Enstatite–sapphirine crack-related assemblages in ultrahigh-pressure pyrope megablasts, Dora-Maira massif, western Alps, *Contrib. Mineral. Petrol.,* 2001, vol. 140, pp. 422–440.

Simon, G., Chopin, C., and Schenk, V., Near-end-member magnesiochloritoid in prograde-zoned pyrope, Dora-Maira massif, western Alps, *Lithos,* 1997, vol. 41, pp. 37–57.

Spear, F.S., Phase equilibria of amphibolites from the Post Pond volcanics, Vermont, *Year Book – Carnegie Inst. Washington,* 1977, vol. 76, pp. 613–619.

Spear, F.S., Petrogenetic grid for amphibolites from the Post Pond and Ammonoosuc volcanics, *Year Book – Carnegie Inst. Washington,* 1978, vol. 77, pp. 805–808.

Spear, F.S., The gedrite–anthophyllite solvus and the composition limits of orthoamphibole from the Post Pond volcanics, Vermont, *Am. Mineral.,* 1980, vol. 65, nos. 11–12, pp. 1103–1118.

Spear, F.S., Phase equilibria of ampibolites from the Post Pond volcanics, Mt. Cube Quadrangle, Vermont, *J. Petrol.,* 1982, vol. 23, pp. 383–426.

Thompson, A., Calc-silicate diffusion zones between marble and pelitic schist, *J. Petrol.,* 1975, vol. 16, pp. 314–346.

Tsujimori, T. and Liou, J.G., Metamorphic evolution of kyanite–staurolite-bearing epidote-ampibolite from the Early Palaeozoic Oeyama Belt, SW Japan, *J. Metamorph. Geol.,* 2004, vol. 22, pp. 301–313.

Tsunogae, T. and Santosh, M., Sapphirine and corundum-bearing granulites from Karur, Madurai Block, Southern India, *Gondwana Res.,* 2003, vol. 6, pp. 925–930.

Tsunogae, T. and van Reenen, D.D., High-pressure and ultrahigh-temperature granulite-facies metamorphism of Precambrian high-grade terranes: case study of the Limpopo Complex, *Mem. Geol. Soc. Amer.,* 2011, vol. 207, pp. 107–124,

Ward, C.M., Magnesium staurolite and green chromian staurolite from Fiordland, New Zealand, *Am. Mineral.,* 1984, vol. 69, pp. 531–540.

White, R.W., Powell, R., Holland, T.J.B., and Worley, B.A., The effect of TiO_2 and Fe_2O_3 on metapelitic assemblages at greenschist and ampibolite facies conditions: mineral equilibria calculations in the system K_2O–FeO–MgO–Al_2O_3–SiO_2–H_2O–TiO_2–Fe_2O_3, *J. Metamorph. Geol.,* 2000, vol. 18, pp. 497–511.

Whitney, D.L. and Evans, B.W., Abbreviations for names of rock-forming minerals, *Am. Mineral.,* 2010, vol. 95, pp. 185–187.

Translated by E. Kurdyukov